ARTICLE

A form of muscular dystrophy associated with pathogenic variants in *JAG2*

Sandra Coppens,[1] Alison M. Barnard,[2] Sanna Puusepp,[3,4] Sander Pajusalu,[3,4] Katrin Õunap,[3,4] Dorianmarie Vargas-Franco,[5] Christine C. Bruels,[5] Sandra Donkervoort,[6] Lynn Pais,[7,8] Katherine R. Chao,[7,8] Julia K. Goodrich,[7,8] Eleina M. England,[7,8,9] Ben Weisburd,[7,8] Vijay S. Ganesh,[7,8,10] Sanna Gudmundsson,[7,8,9] Anne O'Donnell-Luria,[7,8,9] Mait Nigul,[11] Pilvi Ilves,[4,11] Payam Mohassel,[6] Teepu Siddique,[12] Margherita Milone,[13] Stefan Nicolau,[13] Reza Maroofian,[14] Henry Houlden,[14] Michael G. Hanna,[14] Ros Quinlivan,[14] Mehran Beiraghi Toosi,[15] Ehsan Ghayoor Karimiani,[16,17] Sabine Costagliola,[18] Nicolas Deconinck,[19] Hazim Kadhim,[20] Erica Macke,[21] Brendan C. Lanpher,[21,22] Eric W. Klee,[21,22] Anna Łusakowska,[23] Anna Kostera-Pruszczyk,[23] Andreas Hahn,[24] Bertold Schrank,[25] Ichizo Nishino,[26] Masashi Ogasawara,[26]

(Author list continued on next page)

Summary

JAG2 encodes the Notch ligand Jagged2. The conserved Notch signaling pathway contributes to the development and homeostasis of multiple tissues, including skeletal muscle. We studied an international cohort of 23 individuals with genetically unsolved muscular dystrophy from 13 unrelated families. Whole-exome sequencing identified rare homozygous or compound heterozygous *JAG2* variants in all 13 families. The identified bi-allelic variants include 10 missense variants that disrupt highly conserved amino acids, a nonsense variant, two frameshift variants, an in-frame deletion, and a microdeletion encompassing *JAG2*. Onset of muscle weakness occurred from infancy to young adulthood. Serum creatine kinase (CK) levels were normal or mildly elevated. Muscle histology was primarily dystrophic. MRI of the lower extremities revealed a distinct, slightly asymmetric pattern of muscle involvement with cores of preserved and affected muscles in quadriceps and tibialis anterior, in some cases resembling patterns seen in *POGLUT1*-associated muscular dystrophy. Transcriptome analysis of muscle tissue from two participants suggested misregulation of genes involved in myogenesis, including *PAX7*. In complementary studies, *Jag2* downregulation in murine myoblasts led to downregulation of multiple components of the Notch pathway, including *Megf10*. Investigations in *Drosophila* suggested an interaction between *Serrate* and *Drpr*, the fly orthologs of *JAG1/JAG2* and *MEGF10*, respectively. *In silico* analysis predicted that many Jagged2 missense variants are associated with structural changes and protein misfolding. In summary, we describe a muscular dystrophy associated with pathogenic variants in *JAG2* and evidence suggests a disease mechanism related to Notch pathway dysfunction.

Introduction

To date, over 30 genes have been associated with limb-girdle muscular dystrophy (LGMD). The number of genetic subtypes has expanded so rapidly in recent years that the classification system has had to be revised.[1] Similarly, over a dozen genes have been described to date for congenital muscular dystrophy (CMD).[2] Despite the explosion in genetic knowledge for these categories of disease and extensive analyses in clinical research laboratories, a

[1]Center of Human Genetics, Université Libre de Bruxelles, 1070 Brussels, Belgium; [2]Department of Physical Therapy, University of Florida College of Public Health and Health Professions, Gainesville, FL 32610, USA; [3]Department of Clinical Genetics, United Laboratories, Tartu University Hospital, Tartu 50406, Estonia; [4]Institute of Clinical Medicine, University of Tartu, Tartu 50406, Estonia; [5]Division of Pediatric Neurology, Department of Pediatrics, University of Florida College of Medicine, Gainesville, FL 32610, USA; [6]Neuromuscular and Neurogenetic Disorders of Childhood Section, Neurogenetics Branch, NINDS, NIH, Bethesda, MD 20892, USA; [7]Broad Center for Mendelian Genomics, Program in Medical and Population Genetics, Broad Institute of MIT and Harvard, Cambridge, MA 02142, USA; [8]Analytic and Translational Genetics Unit and Center for Genomic Medicine, Massachusetts General Hospital, Boston, MA 02114, USA; [9]Division of Genetics and Genomics, Boston Children's Hospital, Harvard Medical School, Boston, MA 02115, USA; [10]Department of Neurology, Brigham & Women's Hospital and Harvard Medical School, Boston, MA 02115, USA; [11]Department of Radiology, Tartu University Hospital, Tartu 50406, Estonia; [12]Department of Neurology, Feinberg School of Medicine, Northwestern University, Chicago, IL 60611, USA; [13]Department of Neurology, Mayo Clinic, Rochester, MN 55905, USA; [14]Department of Neuromuscular Disorders, University College London Institute of Neurology, London WC1E 6BT, UK; [15]Pediatric Neurology Department, Ghaem Hospital, Mashhad University of Medical Sciences, Mashhad 9176999311, Iran; [16]Molecular and Clinical Sciences Institute, St. George's, University of London, Cranmer Terrace, London SW17 0RE, UK; [17]Innovative Medical Research Center, Mashhad Branch, Islamic Azad University, Mashhad 9187147578, Iran; [18]Institut de Recherche Interdisciplinaire en Biologie Humaine et Moleculaire, Université Libre de Bruxelles, 1070 Brussels, Belgium; [19]Centre de Référence Neuromusculaire and Paediatric Neurology Department, Hôpital Universitaire des Enfants Reine Fabiola, Université Libre de Bruxelles, 1020 Brussels, Belgium; [20]Neuropathology Unit, Department of Anatomic Pathology and Reference Center for Neuromuscular Pathology, Brugmann University Hospital-Children's Hospital, Université Libre de Bruxelles, 1020 Brussels, Belgium; [21]Center for Individualized Medicine, Mayo Clinic, Rochester, MN 55905, USA; [22]Department of Clinical Genomics, Mayo Clinic, Rochester, MN 55905, USA; [23]Department of Neurology, Medical University of Warsaw, 02-091 Warsaw, Poland; [24]Department of Child Neurology, Justus-Liebig-University Giessen, 35390 Giessen, Germany; [25]Department of Neurology, DKD HELIOS Klinik Wiesbaden, 65191 Wiesbaden, Germany; [26]Department of Neuromuscular Research, National Institute of Neuroscience, National Center of Neurology and Psychiatry, Tokyo 187-8551, Japan; [27]Myo-Care Neuromuscular Center,

(Affiliations continued on next page)

Rasha El Sherif,[27] Tanya Stojkovic,[28,29] Isabelle Nelson,[29] Gisèle Bonne,[29] Enzo Cohen,[29] Anne Boland-Augé,[30] Jean-François Deleuze,[30] Yao Meng,[31] Ana Töpf,[32] Catheline Vilain,[1] Christina A. Pacak,[33,34,35] Marie L. Rivera-Zengotita,[36] Carsten G. Bönnemann,[6] Volker Straub,[32] Penny A. Handford,[31] Isabelle Draper,[37] Glenn A. Walter,[38] and Peter B. Kang[5,34,35,39,*]

significant proportion of affected individuals remain without a genetic diagnosis.[3–5] Thus, it is expected that additional associated genes have yet to be identified for these muscular dystrophies.

The Notch signaling pathway is a highly conserved cell-to-cell communication pathway contributing to cell fate decisions during the development and homeostasis of multiple tissues, including skeletal muscle.[6,7] *JAG2* (MIM: 602570) encodes Jagged2, a Notch ligand that has not previously been associated with a human Mendelian disease. Jagged2 is a member of the Notch ligand family that also includes Jagged1, Delta-like protein 1, Delta-like protein 3, and Delta-like protein 4, encoded by *JAG1* (MIM: 601920), *DLL1* (MIM: 606582), *DLL3* (MIM: 602768), and *DLL4* (MIM: 605185), respectively. Notch ligands are transmembrane proteins that share similar extracellular domains, each containing an N-terminal C2 domain, a Delta/Serrate/Lag-2 (DSL) domain, and a variable number of epidermal growth factor (EGF) repeats.[8] Notch ligands interact directly with Notch receptors located on adjacent cells (*trans* interaction), leading to the cleavage of the intracellular domain of the Notch receptor (NICD) that migrates to the nucleus to activate the transcription of target genes. In addition to *trans*-activating interactions, Notch ligands and receptors located on the same cell can establish *cis*-inhibitory interactions.[9]

Dominant, heterozygous truncating, or missense mutations in Notch ligands can cause severe congenital disorders, including the *JAG1*-associated Alagille syndrome 1 (AGS [MIM: 118450]); tetralogy of Fallot (TOF [MIM: 187500]); deafness, congenital heart defects, and posterior embryotoxon (DCHE [MIM: 617992]); peripheral neuropathy; *DLL1*-associated neurodevelopmental disorder with nonspecific brain abnormalities and with or without seizures (NEDBAS [MIM: 618709]); and *DLL4*-associated Adams-Oliver syndrome 6 (AOS6 [MIM: 616589]).[10–15] The *DLL3*-associated autosomal recessive spondylocostal dysostosis (SCDO1 [MIM: 277300]) is caused by bi-allelic *DLL3* pathogenic variants.[16]

JAG2 is located at chromosomal region 14q32.33, comprises 26 exons, and is constrained for predicted loss-of-function (pLoF) variants in the gnomAD. Four pLOF variants are observed in ~150,000 individuals; the expected number for this gene is 64.[17] Among human adult tissues, *JAG2* mRNA is highly expressed in skeletal muscle, heart, and pancreas.[18] The major isoform of the Jagged2 protein has 1,238 amino acids.

Here, we describe 23 individuals, representing 13 unrelated families, with muscular dystrophy and rare bi-allelic *JAG2* variants. Several of the affected individuals have dystrophic muscle biopsy findings and a selective pattern of fatty replacement on muscle magnetic resonance imaging (MRI). Aspects of the phenotype data, muscle transcriptome sequencing, and studies in murine myoblasts and *Drosophila* suggest shared disease mechanisms with early-onset myopathy, areflexia, respiratory distress, and dysphagia (EMARDD [MIM: 614399]) and LGMD R21 *POGLUT1*-related (MIM: 617232).[19,20]

Material and methods

Informed consent, ethics approval, and phenotype data

Informed consent was received from the participants in compliance with protocols approved by the institutional review board (IRB) or equivalent ethics committee of each of the following institutions: Erasme Hospital, Brussels (#P2015/158); University of Florida (#201400469 and #201602123); University of Tartu, Estonia (#187/M-15); National Institute of Neurological Disorders and Stroke, National Institutes of Health (#12-N-0095); University College London Hospitals (#07/Q0512/26); Mayo Clinic (#12-009346 and #13-007054); the National Center of Neurology and Psychiatry, Tokyo (#A2019-123); and the Myo-Care National Foundation (#2-11163). Families GER and POL were consented and enrolled in the MYO-SEQ project, approved by National Research Ethics Service (NRES) Committee North East–Newcastle and North Tyneside 1 (#08/H0906/28).[5] Family FRA was consented and enrolled in the MYOCAPTURE project. Portions of the collaborative team and cohort were assembled via electronic introductions after postings on Matchmaker Exchange[21] and the remainder by direct introductions between collaborators. Demographic, clinical, and genetic data were collected and shared. Clinical data included photographs and reports from muscle biopsies. Muscle MRI studies were obtained either on a research basis or diagnostic basis depending on the site. DNA samples were

Myo-Care National Foundation, Cairo 11865, Egypt; [28]APHP, Nord-Est/Ile-de-France Neuromuscular Reference Center, Myology Institute, Pitié-Salpêtrière Hospital, 75013 Paris, France; [29]Sorbonne Université, INSERM, Center of Research in Myology, UMRS974, 75651 Paris Cedex 13, France; [30]Université Paris-Saclay, CEA, Centre National de Recherche en Génomique Humaine, 91057 Evry, France; [31]Department of Biochemistry, University of Oxford, Oxford OX1 3QU, UK; [32]John Walton Muscular Dystrophy Research Centre, Newcastle University and Newcastle Hospitals NHS Foundation Trust, Newcastle upon Tyne NE1 3BZ, UK; [33]Department of Pediatrics, University of Florida College of Medicine, Gainesville, FL 32610, USA; [34]Paul and Sheila Wellstone Muscular Dystrophy Center, University of Minnesota Medical School, Minneapolis, MN 55455, USA; [35]Department of Neurology, University of Minnesota Medical School, Minneapolis, MN 55455, USA; [36]Department of Pathology, University of Florida College of Medicine, Gainesville, FL 32610, USA; [37]Molecular Cardiology Research Institute, Tufts Medical Center, Boston, MA 02111, USA; [38]Department of Physiology and Functional Genomics, University of Florida College of Medicine, Gainesville, FL 32610, USA; [39]Institute for Translational Neuroscience, University of Minnesota Medical School, Minneapolis, MN 55455, USA
*Correspondence: pkang@umn.edu
https://doi.org/10.1016/j.ajhg.2021.03.020.

obtained from available affected individuals and informative first-degree relatives.

Muscle MRI

Lower extremity MRI studies were performed in eleven participants via the scan sequences and imaging systems available locally (1.5 and 3.0 Tesla Philips and Siemens scanners). To highlight fatty tissue replacement in muscles, we used a number of different MRI sequences. We performed a 3D chemical shift-encoded (Dixon) imaging sequence by using two echo times and reconstructed images to produce fat signal-only images. 2D, T1-weighted whole-body imaging was also obtained for some participants, providing contrast that reveals patterns of muscle fatty replacement. MRIs were acquired in the transverse plane at the pelvis, upper leg, and lower leg levels. Imaging systems and scan sequences are detailed in Table S1.

Exome sequencing

Whole-exome sequencing (WES) was performed in the proband of each family except for families BEL, US1, EST, and UK1, for whom trio-WES was performed. Details about WES platforms and analysis pipelines are provided in Table S2. Segregation analysis was performed by Sanger sequencing.

JAG2 variant reporting and initial analysis

JAG2 variants were numbered according to the GenBank reference transcripts GenBank: NM_002226.5 and NP_002217.3. The gnomAD and Combined Annotation Dependent Depletion (CADD) databases were interrogated for each variant. We found protein sequences of Jagged2 orthologs in Uniprot and aligned them by using the multiple sequence alignment tool Clustal Omega to assess conservation of amino acids across species. Pathogenicity predictions for missense variants were determined with SIFT, PolyPhen2, FATHMM, PROVEAN, and MutationTaster. The schematic representation of Jagged2 domains was created with Illustrator for Biological Sequences (IBS). We created a diagram illustrating the structure of the C2 domain of Jagged2 by uploading the crystal structure of the N-terminal portion of the protein (PDB: 5MW5), from the C2 domain to the second EGF domain, to PyMol (Schrödinger).

Analysis of potential shared haplotypes

To determine whether shared haplotypes were present, we examined variants that passed Variant Quality Score Recalibration (VQSR) filtration (genotype quality $>$ 20 and allele balance $>$ 0.25), had allele frequencies $<$ 5%, and were present within a 2 Mb window centered around the p.Gly839Arg and p.Pro682Ser variants. We included variants shared between the affected participants and heterozygous carriers from the gnomAD v.3.0 database to evaluate the presence of a shared haplotype.

Muscle transcriptome (RNA-seq) analysis

RNA was extracted from vastus lateralis muscle samples obtained from EST.II.1 and US1.II.1. Human whole-transcriptome sequencing was performed by the Genomics Platform at the Broad Institute of MIT and Harvard. The transcriptome product combines poly(A)-selection of mRNA transcripts with strand-specific cDNA library preparation with a mean insert size of 550 bp. Libraries were sequenced on the HiSeq 2500 platform to a minimum depth of 50 million STAR-aligned reads. External RNA Controls Consortium (ERCC) RNA spike-in control mixes were included for all samples, allowing additional control of variability between samples. We used STAR (v.2.5.3) aligner[22] to map sequencing reads to the hg38 reference genome. We used GENCODE v.26[23] to define genes and transcripts. STAR-generated reads per gene counts were used as an input for expression outlier detection with R package OUTRIDER.[24] To detect expression outliers, the muscle biopsy RNA-sequencing (RNA-seq) results were compared with skeletal muscle RNA-seq data from 12 individuals with other myopathies and 100 control individuals from GTEx (dbGaP: phs000424.v8.p2). We calculated gene expression alterations (log2 fold changes) by comparing the normalized read counts for each sample and gene to normalized mean read counts from all affected and control individuals. p values were first calculated on the basis of the fitted negative binomial model and then adjusted via the Benjamini-Yekutieli false-discovery rate method. Statistical significance was determined with adjusted p values with a cutoff of 0.05.

Myoblast culture and shRNA knockdown of *Jag2*

Murine myoblasts (C2C12 cells) were cultured in DMEM with 10% fetal bovine serum and 1% penicillin/streptomycin. At 70%–80% confluence, cells were transfected with the following cocktail of mouse short hairpin RNAs (shRNAs, Genecopoeia): GCAAAGAAGCCGTGTGTAAAC, GCCAAATCAACATCAACGATT, and GCACACATAACACCAATGACT. The following scrambled shRNA sequence was used as a control: CGATACTGAACGAATCGAT. The shRNAs were inserted into a psi-U6.1 vector containing the GFP reporter gene, ampicillin resistance gene for positive selection, and puromycin gene as a stable selection marker. Cell transfection was performed with Lipofectamine 3000 (Thermo Fisher Scientific), including 3.75 μL of transfection reagent and a plasmid DNA concentration of 1,000 ng/μL. We observed GFP expression at 48 h after transfection to determine transfection efficiency. At 48 h, the media was changed to DMEM with 10% fetal bovine serum and 4 μg/mL puromycin for establishment of the stable cell line according to the kill curve.

Quantitative RT-PCR and Notch pathway array of *Jag2*- and scrambled shRNA-treated stable cell lines

Total RNA was extracted from stable *Jag2* shRNA- and scrambled shRNA-treated C2C12 cells via the Quick-RNA miniprep kit (Zymo Research; Cat. No. R1054). RNA concentration and purity were measured with a NanoDrop spectrophotometer (Thermo Fisher Scientific). We then converted RNA into cDNA by using SuperScript IV Vilo Master Mix with ezDNase Enzyme (Thermo Fisher Scientific; Cat. No. 11766050). Quantitative RT-PCR was performed with the TaqMan Fast Advanced Master Mix (Thermo Fisher Scientific; Cat. No. 4444557). The TaqMan probes used for the analysis were pre-designed to target murine *Jag2* (Mm01325629_m1), *Megf10* (Mm01257625_m1), and *Notch1* (Mm00627185_m1) (Thermo Fisher Scientific). Transcript levels were normalized to 18S (probe Mm03928990_g1) via the ΔΔCT method. We designed the experiment with three biological and three technical replicates to validate the results ($n = 3$). The cDNA samples were also examined via the TaqMan Array Mouse Notch Signaling Pathway, Fast 96-well plate (Thermo Fisher Scientific; Cat. No. 4413255) containing a set of Notch signaling pathway-associated genes and endogenous control genes. The Notch arrays were run six times for the *Jag2* shRNA myoblasts and four times for the scrambled shRNA myoblasts. String analysis was performed on the set of genes

Table 1. Clinical features of individuals with Jagged2 pathogenic variants

Family	BEL		IRA	US3	EST	US1	FRA	US2		POL		
Individual n°	II.1	II.2	II.1	II.2	II.1	II.1	II.1	II.1	II.3	II.3	II.4	II.5
Sex, age (years)	F, 13	F, 9	M, 8	M, 5	F, 11	M, 41	M, 22	F, 25	F, 22	F, 53	F, 44	M, 40
Country (origin)	Morocco		Iran	USA	Estonia	USA	France	USA		Poland		
Jagged2 variants	p.[Ala243Asp]; [Ala243Asp]		p.[Glu164Lys]; [Glu164Lys]	p.[Arg165*]; [Trp415Cysfs*11]	p.[Thr95Ala]; [Arg825Cys]	p.[Gly839Arg]; [14q32.33del]	p.[Phe977Ser]; [Phe977Ser]	p.[Cys74Ser]; [Gly839Arg]		p.[Gly839Arg]; [Gly839Arg]		
Onset	infancy (DMM)	infancy (DMM)	infancy (DMM)	infancy (DMM)	childhood	childhood	childhood	adolescence	adolescence	young adult	young adult	young adult
PUL weakness	++	++	++	+	++	++	++/+++	+/++	+	++	+	+
DUL weakness	++	+	++	+	+	–	+/++	–	–	+	–	–
PLL weakness	+++	++/+++	++/+++	+	++	+++	+++	++/+++	++/+++	++/+++	++/+++	++/+++
DLL weakness	+++	++	++	+	+	–	++	–	+	+	+	+
Progression	rapid	rapid	rapid	stable	slow	slow	rapid	slow	slow	slow	slow	slow
LoA (years)	Y (8)	Y (8)	Y (5)	N	N	N	Y (14)	N	N	N	N	N
Contractures	E/A	A	A	–	E/A	S/E/F/K/A	S/E/W/F/K/A	A	A	–	–	–
Muscle trophism	normal	normal	normal	normal	Atr prox > distal	Atr generalized	Atr generalized	normal	normal	normal	normal	Htr Calf
Facial weakness	+	–	–	–	–	+	–	–	–	–	–	–
Ptosis	–	–	–	–	–	+	–	–	–	+	–	–
Neck weakness	+++	++	+	+++	+	+	++	+	++	++	++	+
Scoliosis	+	–	+	–	+	+	+	–	–	–	–	–
Rigid spine	–	–	–	–	–	spine	spine	–	–	–	–	–
FVC (% predicted)	57%	58%	ND	normal	Normal	74%	55%	normal	normal	66%	77%	84%
ID/SD/ASD	moderate ID		–	SD	–	SD	mild ID	SD	–	–	–	–
CK (xULN)	1.3x	ND	normal	normal	1.5x	4x	normal	2x	2.5x	normal	normal	1.1x
EMG	myopathic	ND	myopathic	myopathic	myopathic	myopathic	myopathic	myopathic	myopathic	myopathic	myopathic	ND
Muscle biopsy	dystrophic	ND	dystrophic	dystrophic	dystrophic	dystrophic	dystrophic	dystrophic	dystrophic	ND	dystrophic	ND

(*Continued on next page*)

Table 1. ***Continued***

Family	BEL		IRA	US3	EST	US1	FRA	US2		POL		
Cardiac disease	–	–	–	–	mitral valve prolapse (non-significant)	–	–	–	–	–	–	myocarditis PSVT, AV block (PM at 36 years)
Family	UK		UK2		GER			UAE	EGY			Summary
Individual n°	II.1	II.2	II.1	II.2	II.1	II.2	II.4	II.4	II.1	II.2	II.3	N/A
Sex, age (years)	F, 35	M, 45	F, 21	M, 21	M, 38	M, 36	M, 31	M, 31	F, 27	M, 26	M, 18	F: 11 M: 12
Country (origin)	UK		UK		Sri Lanka			UAE	Egypt			N/A
Jagged2 variants	p.[Pro682Ser]; [Pro682Ser]		p.[Val1050Profs*322]; [Asp702del]		p.[Arg712Cys]; [Arg712Cys]			p.[Pro682Ser]; [Pro682Ser]	p.[Asn358Ile]; [Asn358Ile]			N/A
Onset	childhood	infancy (DMM)	early childhood	childhood	childhood	childhood	childhood	young adult	adolescence			N/A
PUL weakness	++	+	+++	++	+++	+/++	++/+++	++	+/++	+	+	23/23
DUL weakness	++	++	+	+	+	+	+	++	–	–	–	15/23
PLL weakness	+++	++	+++	+++	+++	++/+++	++/+++	++	++/+++	++	+	23/23
DLL weakness	++	++	++	++	+	+	+	++	–	–	–	18/23
Progression	slow	slow	rapid	rapid	rapid	slow	slow	slow	slow	slow	slow	22/23
LoA (years)	N	N	Y (8)	Y (11)	Y (9)	N	Y (18)	N	N	N	N	8/23
Contractures	–	–	A	A	S/E/H/K/A	–	E/H/K/A	–	A	–	–	13/23
Muscle trophism	Htr LL	Htr LL	Atr generalized	Atr generalized	Atr PUL/ DLL/neck	Atr PUL/ DLL/neck	Atr PUL/ DLL/neck	–	Htr calf	Htr calf	Htr calf	Atr 8/23, Htr 6/23
Facial weakness	–	–	–	–	+	+	–	–	–	–	–	4/23
Ptosis	+	+	–	–	–	–	–	–	–	–	–	4/23
Neck weakness	+	+	+	+	+	+	+	+	–	–	–	19/23
Scoliosis	+	+	+	+	+	+	–	+	–	–	–	12/23
Rigid spine/neck	–	–	spine	spine	spine/neck	spine	spine	–	–	–	–	7/23
FVC (% predicted)	75%–80%	75%–80%	ND	ND	41%	42%	44%	75%–80%	normal	normal	normal	low FVC: 13/20
ID/SD/ASD	–	mild ID	ASD	–	–	–	–	–	–	–	–	8/23

(*Continued on next page*)

Table 1. *Continued*

Family	BEL	IRA	US3	EST	US1	FRA	US2	POL		
CK (xULN)	normal	normal	normal	normal	1.4x	1.1x	normal	normal	3.8x	high:10/22
EMG	normal	normal	myopathic	ND	myopathic	ND	normal	myopathic	myopathic	myopathic: 16/19
Muscle biopsy	ND	ND	dystrophic	ND	dystrophic	ND	ND	ND	IFSV	IFSV	abnormal: 14/14
Cardiac disease	–	WPW (ablation)	cardiomyopathy	cardiomyopathy	–	–	–	–	–	–	5/23

Abbreviations are as follows: F, female; M, male; DMM, delayed motor milestones; Y, yes; N, no; S, shoulders; E, elbows; W, wrists; F, fingers; H, hip; K, knees; A, ankles; ID, intellectual disability; SD, speech delay; ASD, autism spectrum disorder; ND, not done; FVC, forced vital capacity; LoA, loss of ambulation; CK, creatine kinase level; ULN, upper limit of normal; FVC, forced vital capacity; PUL, proximal upper limb; DUL, distal upper limb; LL, lower limb; PLL, proximal lower limb; DLL, distal lower limb; +, mild; ++, moderate; +++, severe; Atr, atrophy; Htr, hypertrophy; PSVT, paroxysmal supraventricular tachycardia; AV block, atrioventricular block; PM, pacemaker; WPW, Wolff-Parkinson-White syndrome; IFSV, increased fiber size variability.

that were differentially regulated to statistically significant degrees.[25]

Drosophila stocks and culture

The *UAS-ds drpr* line (genotype: *w1118; P{GD2628}v4833*; stock# 4833) was obtained from the Vienna *Drosophila* Resource Center (VDRC). The *Ser-Gal4* driver line (genotype: *w*; P{Ser-GAL4.GF}1 P{Ser-GAL4.GF}2*; FBst0006791) that expresses Gal4 in the dorsal compartment of wing imaginal discs adjacent to the myogenic layer was obtained from the Bloomington *Drosophila* Stock Center at Indiana University (Bloomington, IN). All stocks were raised at 25°C in a 12 h light/12 h dark cycle on standard *Drosophila* media. To generate RNAi flies that downregulate Drpr in Serrate-positive cells, we crossed transgenics carrying the *UAS-ds drpr* transgene with *Ser-Gal4* driver flies at 29°C (the strength of the yeast-derived *Gal4/UAS* binary system increases with the temperature). We generated control progeny in parallel by crossing the standard genetic background strain w^{1118} (*w* allele FBal0018186) flies with *Ser-Gal4* flies. All adult progeny were collected after emerging, aged, and phenotypically characterized with a negative geotaxis assay (to assess motor activity), as previously described.[26]

Results

Phenotypes

An overview of clinical features of affected family members is presented in Table 1, and pedigrees are presented in Figure 1. The cohort included 12 males and 11 females from 13 unrelated families. Six families were consanguineous, and eight families had multiple affected members. The youngest individual included was 5 years old, and the oldest was 53 years at last evaluation. Onset of muscle weakness occurred during infancy in five affected individuals, childhood in nine affected individuals, and adolescence/young adulthood in nine affected individuals. Limb weakness was present in all affected individuals, and there was lower extremity and proximal dominance. Muscle weakness was progressive in all but one affected individual, and loss of ambulation occurred in eight affected individuals (range: 8–18 years). Axial weakness was a prominent feature, and neck flexion weakness was present in almost all affected individuals. Scoliosis was present in twelve affected individuals, and rigid spine was present in seven. Mild facial weakness was present in four affected individuals and ptosis in four affected individuals, whereas ophthalmoplegia was consistently absent. Joint contractures were described in thirteen affected individuals, muscle atrophy in eight, and muscle hypertrophy in six. Sensory examination was normal in all. Deep tendon reflexes were reduced or absent in most affected individuals. Cardiomyopathy was present in two affected individuals and cardiac arrhythmias in two others. Pulmonary function testing was available in 20 affected individuals and revealed reduced forced vital capacity in 13 of them (range: 41%–84%). None needed respiratory support. No skin abnormality was reported. Four affected individuals had intellectual disability. Their brain MRIs revealed no structural abnormalities. Additionally, one affected

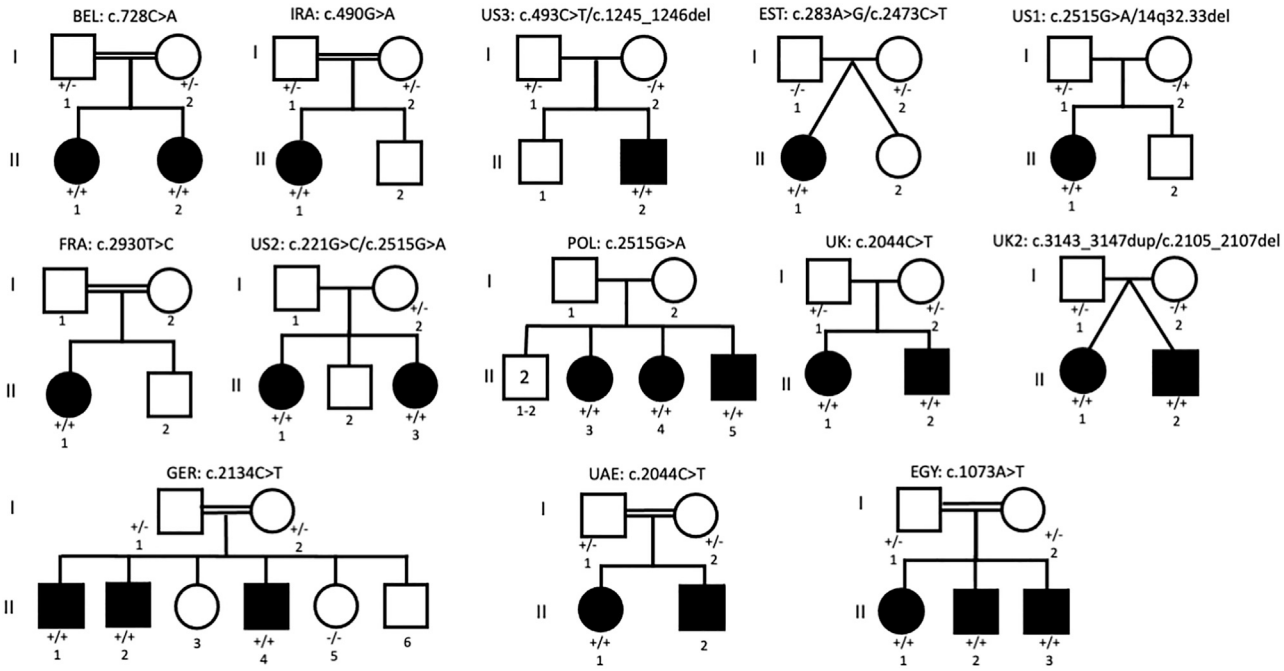

Figure 1. Pedigrees of families with affected individuals and segregation analysis
+, mutated allele; –, normal allele.

individual had autism spectrum disorder and three affected individuals had speech delay. Serum creatine kinase (CK) levels were normal or mildly elevated (<10× upper limit of normal). Electromyography was performed in 19 individuals and revealed a myopathic pattern in 16 and a normal pattern in three others. Nerve conduction studies were normal in all assessed participants except US1.II.1, whose right superficial peroneal and sural sensory nerve studies showed borderline low amplitude responses with normal conduction velocities.

Muscle biopsy findings

Diagnostic skeletal muscle biopsies from 14 affected participants demonstrated a range of myopathic findings, including prominent variation in myofiber size, increased internal nuclei, myofiber splitting, myofiber necrosis and phagocytosis, mild to marked endomysial fibrosis, and various degrees of fatty transformation (Figure 2). Some of the biopsies showed clear dystrophic features. Oxidative stains demonstrated evidence of myofibrillar architecture distortion, including lobulated, whorled, and moth-eaten fibers and myofibers with areas of poorly circumscribed focal losses of oxidative enzyme reactivity, sometimes referred to as core-like areas.

Muscle MRI findings

The 11 participants in this cohort who underwent lower extremity MRI studies were found to have a distinct pattern of muscle involvement on MRI, particularly within the quadriceps muscles of the thigh. In the majority of individuals who underwent imaging, the vastus lateralis, intermedius, and medialis muscles demonstrated fatty transformation that progressed from the outside of the muscle borders inward, often leaving small central areas of less affected muscle (Figure 3, arrows). A similar pattern was also occasionally seen in other muscles, such as the biceps femoris long head and the gluteus medius. The rectus femoris muscle demonstrated either a bullseye type pattern or a focal area of fatty transformation, and these focal areas of degeneration were also seen in the tibialis anterior muscle of the lower leg (Figure 3, arrow heads). No single muscle group appeared to be completely spared, although fatty transformation was markedly more severe in proximal compared with distal muscles, which were only mildly affected. Two siblings (POL.II.4 in Figure 3 and POL.II.3 in Figure S1) had patterns of muscle involvement that differed from the rest of the cohort, primarily in the thigh. These individuals demonstrated less fatty replacement in the outer edge of the vastus lateralis and relative sparing of the rectus femoris and sartorius muscles. In contrast, the patterns of muscle involvement in the lower leg and pelvis of the siblings were more similar to those seen in the other participants.

Genetic findings

The affected individuals in all 13 families harbored homozygous or compound heterozygous variants in *JAG2* that segregated with the phenotype (Figure 4A and Table 2). Fifteen different variants were identified in the cohort: ten missense variants, a nonsense variant, two frameshift variants, an in-frame deletion, and a 14q32.33 deletion encompassing *JAG2*. All variants were either absent or present in the heterozygous state at very low frequencies in gnomAD (except c.2044C>T [p.Pro682Ser], 63 alleles in gnomAD [GenBank: NM_002226.5 and NP_002217.3]). All variants

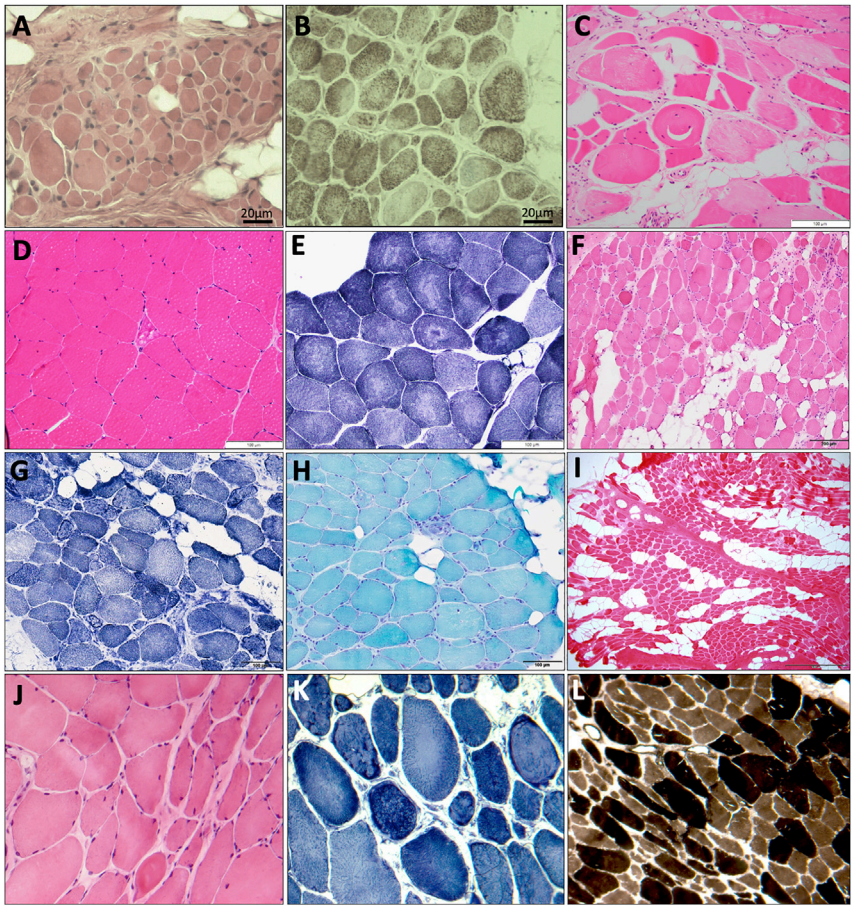

Figure 2. Muscle histology

(A) BEL.II.1, hematoxylin & eosin (H&E)-stained sections illustrating marked variation in myofiber size with both small and large rounded myofibers, occasional internalized nuclei, hypercontracted fibers, and endomysial fibrosis with early fatty replacement. Scale bar, 20 μm.

(B) BEL.II.1, COX-SDH showing myofibers with areas of COX-deficient/absent stain and suggesting myofibrillar architectural changes such as moth-eaten fibers and areas of poorly circumscribed focal losses of oxidative enzyme reactivity, sometimes referred to as core-like areas. Scale bar, 20 μm.

(C) US2.II.1, paraffin-embedded, H&E-stained section of skeletal muscle shows myopathic features, including myofiber size variability, fiber splitting, internalized nuclei, and endomysial fibrosis. Scale bar, 100 μm.

(D) US2.II.3, snap-frozen, H&E-stained section of skeletal muscle shows mild variation in myofiber size with focal individual degenerating myofibers. Scale bar, 100 μm.

(E) US2.II.3, NADH-TR shows myofibers with myofibrillar architecture changes, including core-like areas and moth-eaten fibers. Scale bar, 100 μm.

(F) US1.II.1, H&E demonstrating prominent myopathic/dystrophic features, including marked variability in myofiber size, hypercontracted fibers, endomysial fibrosis, and fatty replacement. Scale bar, 200 μm.

(G) US1.II.1, NADH showing disruption of the myofibrillar architecture such as lobulated fibers and moth-eaten fibers. Scale bar, 100 μm.

(H) US1.II.1, modified Gomori trichrome stain showing variability in myofiber size, scattered fibers undergoing myophagocytosis, as well as increased endomysial and perimysial connective tissue. Scale bar, 100 μm.

(I) EST.II.1, H&E illustrating variation in myofiber size, moderate endomysial fibrosis, and fatty infiltration.

(J) GER.II.1, H&E shows variability in myofiber size, occasional internal nuclei, and endomysial fibrosis.

(K) GER.II.1, NADH demonstrating lobulated and whorled fibers.

(L) GER.II.1, ATPase pH10.4 shows atrophic myofibers of both types and hypertrophic type 2 myofibers.

had CADD scores greater than 20, ranking them among the 1% most deleterious variants predicted in the human genome. The amino acid residues affected by the ten missense variants were all highly conserved (Figure 4B). All variants were predicted to be damaging for protein function by a majority of the following prediction tools: PolyPhen2, SIFT, PROVEAN, FATHMM, and MutationTaster (Table S3). The nonsense variant, c.493C>T (p.Arg165*) (GenBank: NM_002226.5 and NP_002217.3), was located in the fourth exon of *JAG2*, which comprises a total of 26 exons. The frameshift deletion, c.1245_1246delGG (p.Trp415Cysfs*11) (GenBank: NM_002226.5 and NP_002217.3), leads to the appearance of a premature termination codon (PTC) in exon nine. The frameshift duplication, c.3143_3147dup (p.Val1050Profs*322) (GenBank: NM_002226.5 and NP_002217.3), is located in the penultimate exon of *JAG2* and does not lead to the appearance of a PTC but instead to the replacement of the 188 last amino acids of Jagged2, comprising the transmembrane domain, by 322 completely new amino acids. A maternally inherited 3.2 Mb terminal deletion at 14q32.33, encompassing *JAG2,* was observed in family US1 in combination with a paternally inherited missense variant; both parents were unaffected. The deletion was also identified by metaphase fluorescence *in situ* hybridization (FISH) studies via a 14q subtelomere probe (Abbott Molecular). The deleted interval includes 61 known genes (Table S4), including *JAG2*. Two families (UK2.II.1/UK2.II.2 and UAE.II.4) were found to have a homozygous c.2044C>T (p.Pro682Ser) (GenBank: NM_002226.5 and NP_002217.3) variant that was determined to be likely pathogenic; this variant was rare, but 63 heterozygous alleles were present in gnomAD and none were in the homozygous state. The p.Pro682Ser variant was highly conserved, had a CADD score of 27, and was predicted to be damaging by multiple prediction tools. There were no other plausible pathogenic variants in these two families.

In silico analyses to predict effects of amino acid substitutions

To investigate the impact of amino acid substitutions on the structure and/or function of Jagged2, we mapped

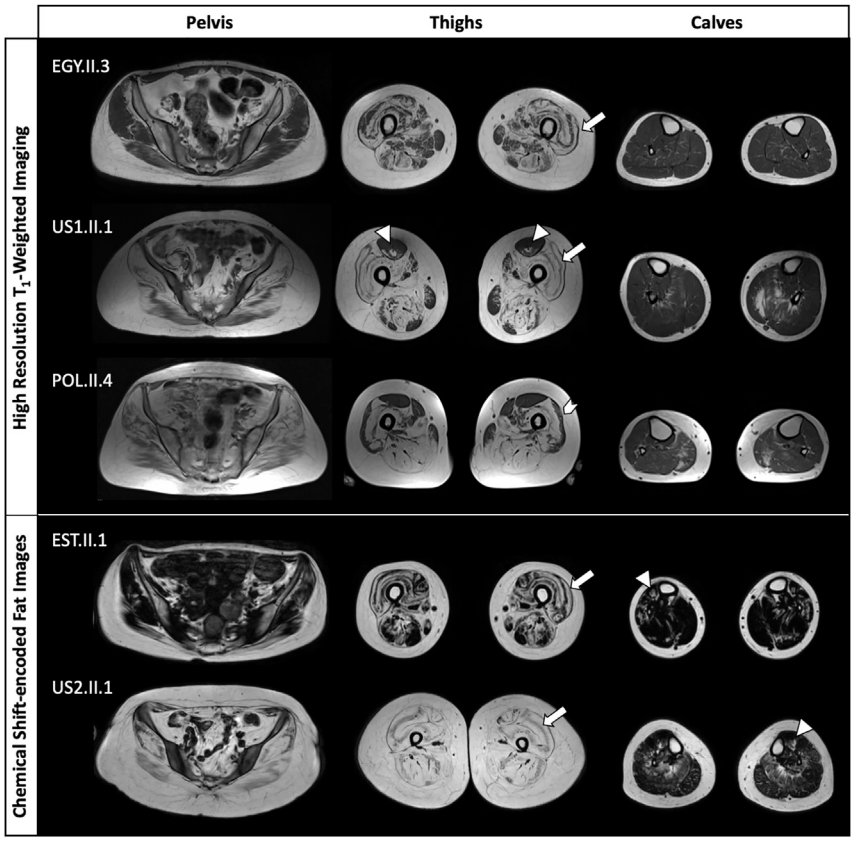

Figure 3. Muscle MRI
Axial T1-weighted imaging and axial fat images derived from chemical shift-encoded imaging reveal distinct patterns of fatty infiltration and muscle involvement in the pelvis and lower extremities in *JAG2*-related muscular dystrophy. Four of the five participants had cores of preserved muscle within the vastus lateralis (arrows), vastus medialis, and vastus intermedius. Focal areas of degeneration (arrow heads) were present in the tibialis anterior and rectus femoris in some cases. In one of the participants imaged (POL.II.4), the pattern of involvement was unique in the vastus lateralis (chevron). While others did not have any muscles that were specifically spared, this individual demonstrated preservation of the rectus femoris and sartorius muscles. A sibling of this individual shares this unique pattern (POL.II.3 in Figure S1).

four substitutions to the crystal structure of Jagged2 (PDB: 5MW5).[8] Three of these substitutions (p.Cys74Ser, p.Thr95Ala, and p.Glu164Lys) (GenBank: NM_002226.5 and NP_002217.3) are located in the N-terminal C2 domain (Figure 4C). The C2 domain has been shown to bind phospholipid, but also has a Notch receptor binding surface, in addition to the site within the DSL domain.[8,27] The structure of the C2 domain is composed of an eight-stranded β sandwich stabilized by three disulfide bonds. The p.Cys74Ser substitution disrupts a disulfide bond formed with Cys88, which is likely to cause C2 domain misfolding. The equivalent p.Cys78Ser substitution in Jagged1 protein has been described as pathogenic in individuals with Alagille syndrome.[28] The Thr95 residue lies in the β3–4 loop of the C2 domain, away from the Notch binding surface. β1–2 and β5–6 loops at the apex of the C2 domain of Jagged proteins are implicated in phospholipid binding that is required for optimal Notch activation, as are other residues in the wider C2 domain family.[8] Substitutions of residues forming the apical loops in Jagged1 are associated with extrahepatic biliary atresia (EHBA [MIM: 210500])[29] and were shown to impair phospholipid recognition, leading to reduced Notch activation.[8] The fourth substitution changes a negatively charged glutamic acid in position 164 to a positively charged lysine (p.Glu164Lys) on a β strand that is part of the structural core and may cause misfolding of the C2 domain. The Ala243 residue is located in the linker sequence between the DSL domain and the first EGF repeat. The substitution of an uncharged alanine residue by a negatively charged aspartic acid (p.Ala243Asp) may disrupt this domain/domain interface.

Five other Jagged2 missense variants (p.Asn358Ile, p.Pro682Ser, p.Arg712Cys, p.Arg825Cys, and p.Gly839Arg) (GenBank: NM_002226.5 and NP_002217.3) lie in EGF repeats 4, 12, 13, 15, and 16. EGF repeats are sequences of 30–40 amino acids stabilized by three disulfide bonds. Two missense variants (p.Arg712Cys and p.Arg825Cys) involve the gain of an additional cysteine residue within the EGF repeat 13 or 15. This could induce the formation of non-native disulfide bonds and disturb folding, as has been described as a pathological mechanism in individuals with Alagille syndrome[28] and Marfan syndrome[30,31] (MIM: 154700). Glycine and proline residues are known to play important structural roles in the formation of the EGF fold.[32] The p.Pro682Ser and p.Gly839Arg substitutions may therefore interfere with native folding of EGF repeats because they disrupt highly conserved residues.

Analysis of potential shared haplotypes

The c.2515G>A (p.Gly839Arg) substitution was the most common variant in the cohort, and it was found in three unrelated families. We assessed whether this variant was present on a shared haplotype with evidence for common ancestry between three families, including two affected sisters (family US2) who are compound heterozygous for this substitution, three affected siblings (family POL) who are homozygous, and one sporadic individual (US1.II.1) who harbors the variant in *trans* with a 14q32.33 microdeletion. Five informative markers (allele frequency of 0.089%, 3.1%, 4.0%, 0.052%, and 0.22%) within 0.6 Mb of the c.2515G>A variant were shared between US1.II.1 individual, the POL family, and three out of eight heterozygous carriers in gnomAD v.3.0, indicating a common haplotype. There was no

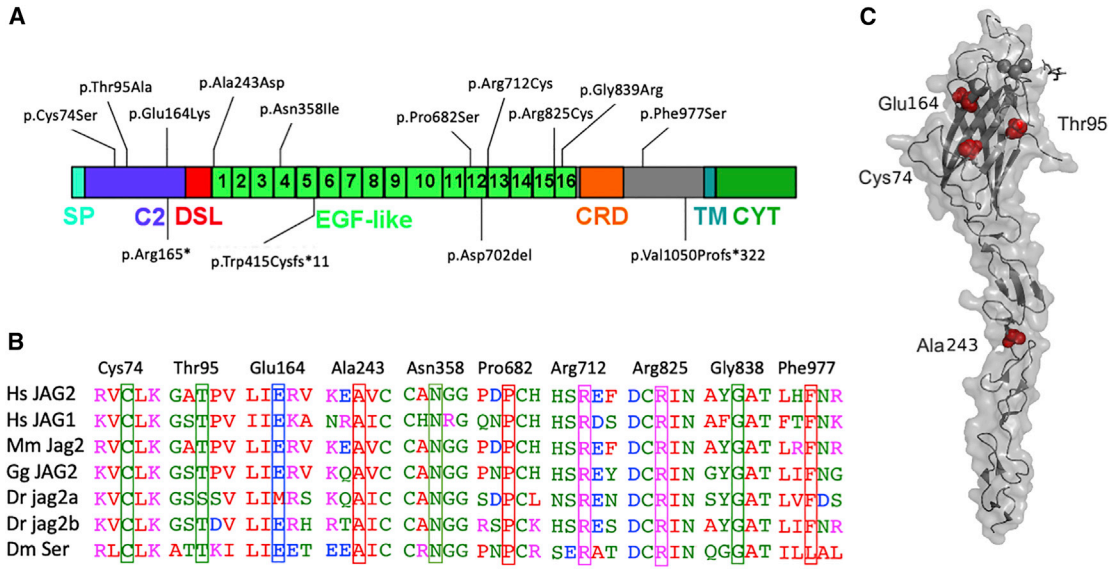

Figure 4. Pathogenic variants in *JAG2* and conservation of substituted residues

(A) Schematic representation of Jagged2 domains and location of the pathogenic variants identified in the cohort. Missense variants are shown above, and frameshift and nonsense variants are shown below the diagram. Domain nomenclature is as follows: SP, signal peptide; DSL, Delta/Serrate/Lag-2 domain; C2, C2 domain; EGF-like, epidermal growth factor-like; CRD: cysteine-rich domain, TM, transmembrane domain; CYT, cytoplasmic domain.

(B) Clustal alignment of human Jagged proteins (Hs JAG2 and Hs JAG1) and Jagged2 orthologs for different animal species. Residues with missense substitutions are surrounded by a rectangle. Species nomenclature is as follows: Hs, *Homo sapiens*; Mm, *Mus musculus*; Gg, *Gallus gallus*; Dr, *Danio rerio*; Dm, *Drosophila melanogaster*.

(C) Muscular dystrophy-associated missense variants (red) are shown in space-filling representation and mapped onto the structure of Jagged-2 N-EGF2 fragment (PDB: 5MW5) comprising C2, DSL, EGF1, and EGF2 (gray diagram and solid surface). Ca^{2+} ions and N-glycan are shown in gray.

evidence of a shared haplotype between the affected sisters (family US2) with any of the gnomAD carriers.

The c.2044C>T (p.Pro682Ser) substitution was present in three individuals from two unrelated families (UK2.II.1/UK2.II.2 and UAE.II.4). These individuals shared 83 variants in a 2 Mb autozygous region including four informative markers (allele frequency 4.8%, 4.3%, 0.09%, and 0.06%), supporting that these probands have a common haplotype. The low number of rare markers in proband exomes limited analysis of a shared haplotype with the 27 gnomAD v.3.0 genome samples heterozygous for c.2044C>T. However, analysis of rare variants shared solely by the 27 population genomes revealed two rare non-coding variants present in all 27 samples, located 4 kb downstream and 31 kb upstream of the *JAG2* c.2044C>T variant (allele frequency 4.7% and 0.03%). One was present in the probands and one was in a non-coding region that was not covered in the probands' exome data. Additionally, 25 of the 27 samples shared 25 markers (allele frequency < 10%) within 0.5 Mb of c.2044C>T, including eight rare markers with an allele frequency of <1%. The large set of shared rare variants suggests that the disease variant is identical by descent in the proband and gnomAD individuals, indicative of a shared haplotype.

Candidate variants in other genes

In individual US3.II.2, a 77 kb Xq24 hemizygous deletion of unclear clinical significance was identified, involving a partial deletion of the gene *LOC101928336*, which encodes an uncharacterized protein. No other plausible alternate pathogenic variants were identified in our genetic analyses.

Muscle transcriptome analysis (RNA-seq)

RNA-seq from skeletal muscle tissue obtained from participant EST.II.1 identified three significant outliers with respect to gene expression in this subject versus control individuals: *PAX7* (p = 3.7e−9, adjusted p value [padj] = 0.00056, $Z = -7.41$, log 2-fold change [l2fc] = 7.16), *MYF5* (p = 1.21e−7, padj = 0.0061, $Z = -7.51$, l2fc = −8.92), and *CADM2* (p = 2.77e−8, padj = 0.0021, $Z = -7.06$, l2fc = 4.45). For US1.II.1, only one gene was noted to be a statistically significant outlier: *PACS2* (p = 2.12e−7, padj = 0.032, $Z = 5.48$, l2fc = −0.93). However, both *PAX7* (p = 2.86e−6, padj = 0.14, $Z = -5.09$, l2fc = 4.97) and *MYF5* (p = 5.93e−5, padj = 1, $Z = -4.58$, l2fc = −5.54) showed decreased expression based on unadjusted p values, albeit not after p value adjustment. Moreover, *PAX7* and *MYF5* downregulation was not observed in 12 other myopathy-affected individuals or in 100 control samples (Figure 5, Table S5, and Table S6).

Effect of *Jag2* knockdown on the Notch pathway in murine myoblasts

Quantitative gene expression analysis of *Jag2*, *Megf10*, and *Notch1* in *Jag2* knockdown experiments in C2C12 cells

Table 2. *JAG2*/Jagged2 variants, exon and domain location, CADD scores, and population frequency

Genomic change (hg19)	CDS change	Amino acid change	Exon (/26)	Domain	CADD score	gnomAD allele count/ other substitution count
chr14: 105634290C>G	c.221G>C	p.Cys74Ser	2	C2	23,1	0
chr14: 105634228T>C	c.283A>G	p.Thr95Ala	2	C2	22,7	1 (Hom = 0)
chr14: 105622312C>T	c.490G>A	p.Glu164Lys	4	C2	24,5	0
chr14: 105621959G>T	c.728C>A	p.Ala243Asp	5	EGF1	27,3	0
chr14: 105618043T>A	c.1073A>T	p.Asn358Ile	8	EGF4	23,4	0 (p. Asn358Ser: 2)
chr14: 105614753G>A^	c.2044C>T	p.Pro682Ser	16	EGF12cb	27,2	63 (Hom = 0)
chr14: 105614690_105614692del	c.2105_2107del	p.Asp702del	16	EGF12cb	N/A	0 (p.Asp702Asn: 2)
chr14: 105614663G>A	c.2134C>T	p.Arg712Cys	16	EGF13	33	0 (p.Arg712Ser: 2, p.Arg812Gly:1)
chr14: 105613669G>A	c.2473C>T	p.Arg825Cys	20	EGF15cb	25,6	0 (p.Arg825His: 2)
chr14: 105613026C>T^	c.2515G>A	p.Gly839Arg	21	EGF16cb	29,4	6 (Hom = 0)
chr14: 105612090A>G	c.2930T>C	p.Phe977Ser	23	–	20,5	0
chr14: 105617641_105617642del	c.1245_1246del	p.Trp415Cysfs*11	9	EGF5	N/A	0
chr14: 105622309G>A	c.493C>T	p.Arg165*	4	N/A	39	2 (Hom = 0)
chr14: 105609913_105609917dup	c.3143_3147dup	p.Val1050Pro fs*322	25	N/A	N/A	0

Abbreviations are as follows: CDS, coding sequence; ^, recurring variant; C2, N-terminal C2 domain; N/A, not applicable; EGF, EGF repeats; cb, calcium binding; Hom, homozygous.

with shRNA showed that reducing *Jag2* expression by ~70% resulted in reduction in *Megf10* expression by ~53% compared with scrambled shRNA-treated cells and no significant changes in *Notch1* expression (Figure 6A). Quantitative Notch pathway gene expression array analysis in *Jag2* knockdown C2C12 cells demonstrated that 22 of 75 measured genes had statistically significant changes in gene expression; all of these genes were downregulated (Figure 6B). Of the 22 significantly altered genes, 14 had 2-fold or greater downregulation of gene expression compared to scrambled shRNA cells. On the basis of string analysis, the downregulated genes that were most closely associated with *Jag2* were *Jag1*, *Dll1*, *Neurl1a*, *Cd44*, and *Ccnd1* (Figure 6C).

Serrate and *Drpr* in *Drosophila*

To assess whether the fly ortholog of *JAG2*, i.e., *Serrate* (*Ser*), acts together with another multiple EGF repeat-containing protein interacting with Notch that underlies muscular dystrophy, i.e., mammalian *MEGF10*/fly *Drpr*, we generated transgenic *Drosophila* that express a *drpr*-RNAi construct in the discrete and well-characterized subset of Ser-positive cells located in the wing imaginal disc (RNAi fly genotype: *Ser-Gal4 > UAS-ds drpr*; control fly genotype: w^{1118}*; Ser-Gal4*). Ser expressed in these epithelial cells is known to activate Notch in the closely opposed adult muscle progenitors (AMPs). Both male and female flies that downregulate Drpr in Ser-positive cells displayed a marked decline in locomotor activity with age (versus corresponding age-matched controls), as assessed in the negative geotaxis assay. The phenotype manifests earlier in males versus females (Figure 7). Some of the RNAi flies are able to fly but their climbing activity is visibly impaired (Video S1).

Discussion

In this study, we report a large international cohort of individuals with muscular dystrophy and bi-allelic *JAG2* variants. A spectrum of severity was evident: some affected individuals experienced onset during infancy and others experienced later onset ranging from childhood to young adulthood. Muscle weakness had a progressive course in most affected individuals and was most prominent in the proximal lower limb and axial muscles; more than half of the individuals had asymptomatic moderate respiratory muscle weakness. Joint contractures, scoliosis, and rigid spine or neck were also frequently noted. Cardiac and cognitive involvement were present in 35% and 17% of the affected individuals, respectively. Muscle biopsies disclosed myopathic or clearly dystrophic features.

The majority of the participants with *JAG2* variants demonstrated a distinct pattern of lower extremity muscle involvement on MRI. The involvement of the quadriceps was the most defining feature, with an inner core of preserved muscle, similar to what is seen with COL6-related muscular dystrophy (Bethlem and Ullrich muscular dystrophy [MIM: 158810 and 254090])[33] and advanced stages of LGMD R1 calpain 3-related (MIM: 253600).[34] In contrast, the pattern of involvement in the calves and pelvis seen in *JAG2*-related muscular dystrophy may help distinguish this entity from COL6-related muscular dystrophy and LGMD R1 calpain 3-related. Additionally, the "target"

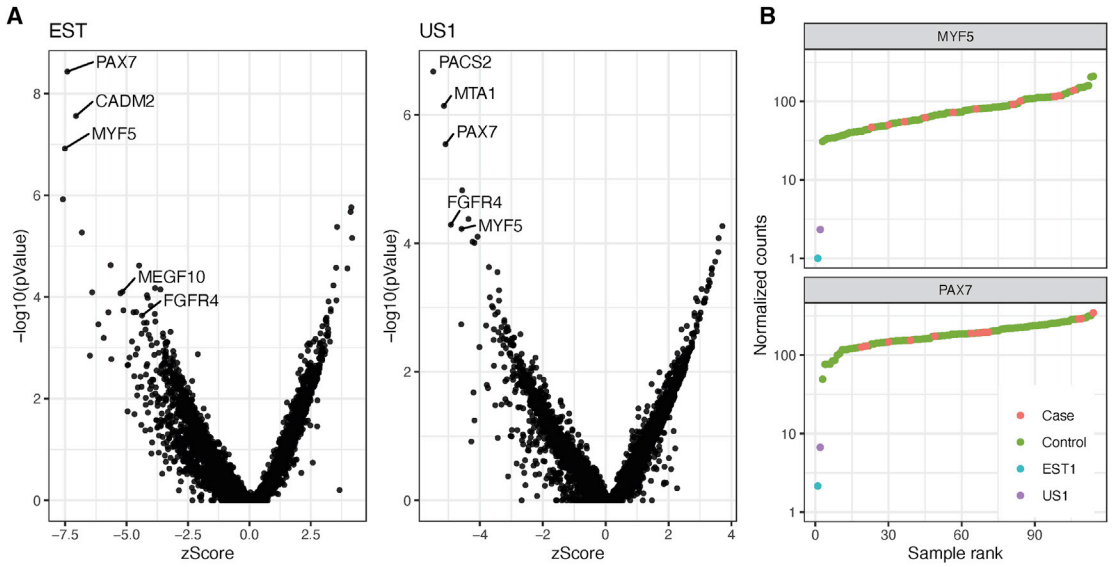

Figure 5. Transcriptome (RNA-seq) results for EST.II.1 and US1.II.1
(A) Volcano plots demonstrating that *MYF5* and *PAX7* are downregulated compared with a set of 100 muscle biopsy controls from the GTEx project and 12 other individuals with various neuromuscular disorders.
(B) EST.II.1 and US1.II.1 show lower normalized read counts on RNA-seq for *MYF5* and *PAX7* compared with other analyzed samples.

sign present in the rectus femoris muscle in COL6-related muscular dystrophy[35] was present in only some cases of *JAG2*-related muscular dystrophy. Two participants with confirmed *JAG2* variants demonstrated unique patterns of involvement, particularly in the femoral quadriceps muscle, with relative sparing of the rectus femoris and sartorius muscles. This pattern in the thigh muscles appears to be consistent with muscle involvement seen in LGMD R21 *POGLUT1*-related. The anatomic and biologic substrates of these imaging findings are currently unknown but bear further study of possible contributing factors, such as patterns of muscle development, metabolism, perfusion, and others.

We observed a correlation between the location of the mutation and the age of onset and severity of weakness. All three individuals with both missense variants located in exons 2 to 5 lost ambulation before the age of 10 years. The majority of *JAG2* variants found in the cohort are predicted to lead to a decrease of Jagged2 expression at the cell surface. Nonsense and frameshift variants introducing premature termination codons are predicted to lead to nonsense-mediated mRNA decay. Many of the missense variants identified are predicted to affect the structure of Jagged2 and a subset is likely to affect the folding of the C2 domain or EGF repeats (Table S7). Misfolded proteins are likely to be at least partially retained in the endoplasmic reticulum where they will be degraded by the endoplasmic reticulum-associated degradation (ERAD) machinery.[36] Other variants, e.g., p.Thr95Ala and p.Ala243Asp, have substitutions that may affect intramolecular or intermolecular interactions, even in the absence of misfolding. Thus, all truncating variants and almost all of the missense variants are expected to cause loss of function.

All affected individuals in the current cohort harbor homozygous or compound heterozygous *JAG2* variants. This contrasts with the heterozygous loss-of-function mutations described for other genes encoding Notch ligands: *JAG1*, *DLL1*, and *DLL4*. The absence of signal amplification steps in the Notch signaling pathway was suggested to lead to this extreme sensitivity to gene dosage for all three genes.[9] In our cohort, numerous unaffected parents were confirmed to be carriers of heterozygous loss-of-function variants in *JAG2*. Why *JAG2* is less sensitive to gene dosage variation than *JAG1*, *DLL1*, and *DLL4* remains an open question. Jagged2 may play a more narrowly defined role in the development of selected organs, such as skeletal muscle and the brain. The recessive pattern of inheritance for pathogenic variants in *DLL3* sets a precedent for this pattern to be seen for other genes encoding Notch ligands, although it should be noted that Delta-like protein 3 is an atypical Notch ligand.[16] Indeed, in contrast to other Notch ligands, Delta-like protein 3 is not expressed primarily at the cell surface and therefore does not activate Notch in *trans*. Instead, Delta-like protein 3 acts as a Notch *cis*-inhibitor by targeting newly synthetized Notch receptors in the Golgi apparatus.[37,38]

Our clinical and biological data indicate potential common disease mechanisms with two other inherited muscle disease-associated genes, *POGLUT1* and *MEGF10*. Autosomal recessive mutations in *POGLUT1*, encoding the protein O-glycosyltransferase 1, an enzyme responsible for the glycosylation of Notch receptors, have been described in individuals with LGMD R21 *POGLUT1*-related.[20,39] As in our cohort, the age of onset is highly variable; weakness is predominantly in the proximal lower limb muscles and it has a slowly progressive course. Respiratory involvement was present in 40% of reported individuals and CK

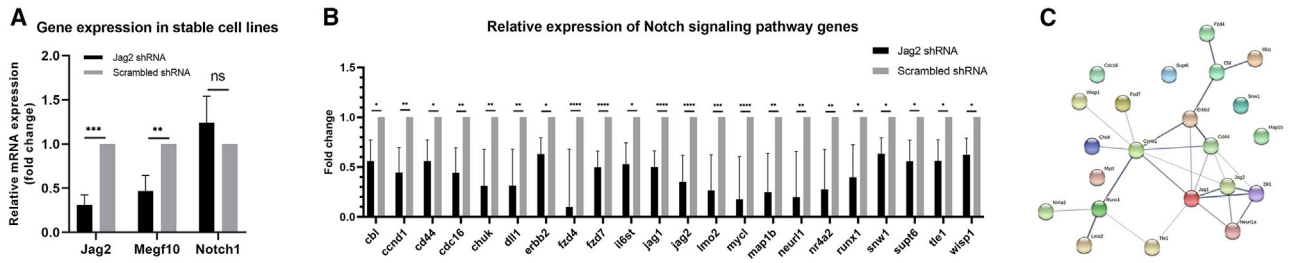

Figure 6. Individual qPCR and Notch array qPCR findings from *Jag2* shRNA-transfected C2C12 cells compared with scrambled shRNA-transfected cells

(A) Bar graph demonstrates the fold changes seen for *Jag2*, *Megf10*, and *Notch1* gene expression. Transcript levels were normalized to 18S via the ΔΔCT method. We designed the experiment with three biological and three technical replicates to validate the results (n = 3). Values in the graph show mean ± standard deviation. We calculated significance by performing unpaired t tests; $p < 0.05$ was considered significant.

(B) Bar graph demonstrates the fold changes seen for 22 Notch pathway genes whose expression levels were significantly different between *Jag2* shRNA-transfected C2C12 cells and scrambled shRNA-transfected cells. Transcript levels were normalized to 18S via the ΔΔCT method. The experiment was designed with six technical replicates for *Jag2*-shRNA C2C12 cells and four technical replicates for scrambled-shRNA C2C12 cells. Results from the replicates of each cell type were averaged for final analysis and determination of fold change in gene expression. Values in the graph show mean ± standard deviation. We calculated significance by performing unpaired t tests; $p < 0.05$ was considered significant.

(C) Illustration of protein-protein interaction networks functional enrichment analysis (STRING analysis) for significantly altered transcripts (22 total). Edges indicate both functional and physical protein associations, and their thickness indicates the strength of data support set at a medium confidence interaction score.

ns, not significant; *$p < 0.05$; **$p < 0.01$; ***$p < 0.001$; ****$p < 0.0001$.

levels were normal or mildly elevated. Autosomal recessive mutations in *MEGF10*, encoding a transmembrane protein that interacts with NOTCH1, were first described in individuals with EMARDD who harbored at least one truncating variant in *MEGF10*.[19] Individuals with bi-allelic missense mutations in *MEGF10* present during early infancy with predominantly proximal and axial muscle weakness. Joint contractures, scoliosis, and prominent neck weakness were also reported. Respiratory failure occurred after the age of 10 years, necessitating nocturnal assisted ventilation. As in our individuals, moth-eaten and core-like areas were noted on muscle biopsies in addition to typical dystrophic features.[40]

Clinically, the three diseases, LGMD R21 *POGLUT1*-related, EMARDD, and *JAG2*-related muscular dystrophy, share several phenotypic features. All three have infantile and later onset forms, a high frequency of respiratory complications (albeit less severe in *JAG2*-related muscular dystrophy), and CK levels that range from normal to mildly elevated. There are similarities in the muscle MRI patterns between LGMD R21 *POGLUT1*-related and *JAG2*-related muscular dystrophy; there are only two reports in the literature of EMARDD that include muscle MRI figures, and a comparison of that limited sample of images does not indicate shared patterns.[41,42] However, there are also parallels between the *MEGF10* and *JAG2*-related diseases with respect to prominent neck flexion weakness and muscle histological features.

Satellite cell dysfunction secondary to impaired Notch signaling was proposed as the disease mechanism implicated in LGMD R21 *POGLUT1*-related and EMARDD,[39,40] and there are indications that this may be true for *JAG2*-related muscular dystrophy as well. Satellite cells are resident muscle stem cells located in a niche between the muscle fiber and the basal lamina.[43] Upon skeletal muscle injury, satellite cells proliferate, migrate, and differentiate to fuse with damaged muscle fibers or to form new muscle fibers. They are crucial for muscle regeneration.[44] The Notch pathway plays an essential role in maintaining the quiescence of satellite cells in uninjured adult muscle. In mice, conditional knockout of Notch pathway components in satellite cells leads to their spontaneous differentiation without self-renewal and finally to a severe depletion of the pool of satellite cells and to a defect of muscle regeneration.[45–47] Although the importance of Notch signaling for satellite cell homeostasis has been clearly demonstrated, important questions remain to be answered. Which member(s) of the Notch ligand family is implicated in this interaction? The GTEx database indicates that *JAG2* and *NOTCH3* are the most highly expressed among Notch ligands and receptors in adult human skeletal muscle. Single-cell RNA-seq of muscle samples from ten human adult donors undergoing surgery revealed a potential interaction between *NOTCH3* in quiescent satellite cells and *DLL4* and *JAG2* in endothelial cells.[48] In addition, mouse experiments have shown that endothelial cells on blood vessels adjacent to muscle satellite cells can provide a Jagged2 ligand-expressing niche for the Notch2/3 receptors expressed on satellite cells.[49]

In individuals EST.II.1 and US1.II.1, muscle RNA-seq suggested diminished expression of *PAX7*, which encodes a key transcription factor expressed by satellite cells.[50] Although only studied in two participant samples, this finding is notable because it potentially ties *JAG2*-related muscular dystrophy with myopathies associated with depletion of satellite cells, including those caused by pathogenic variants in *PAX7*,[51] *SEPN1*,[52] *TRIM32*,[53] *POGLUT1*,[20] and *MEGF10*.[19] In contrast, gene expression microarray data obtained from muscle samples of individuals with certain other types of

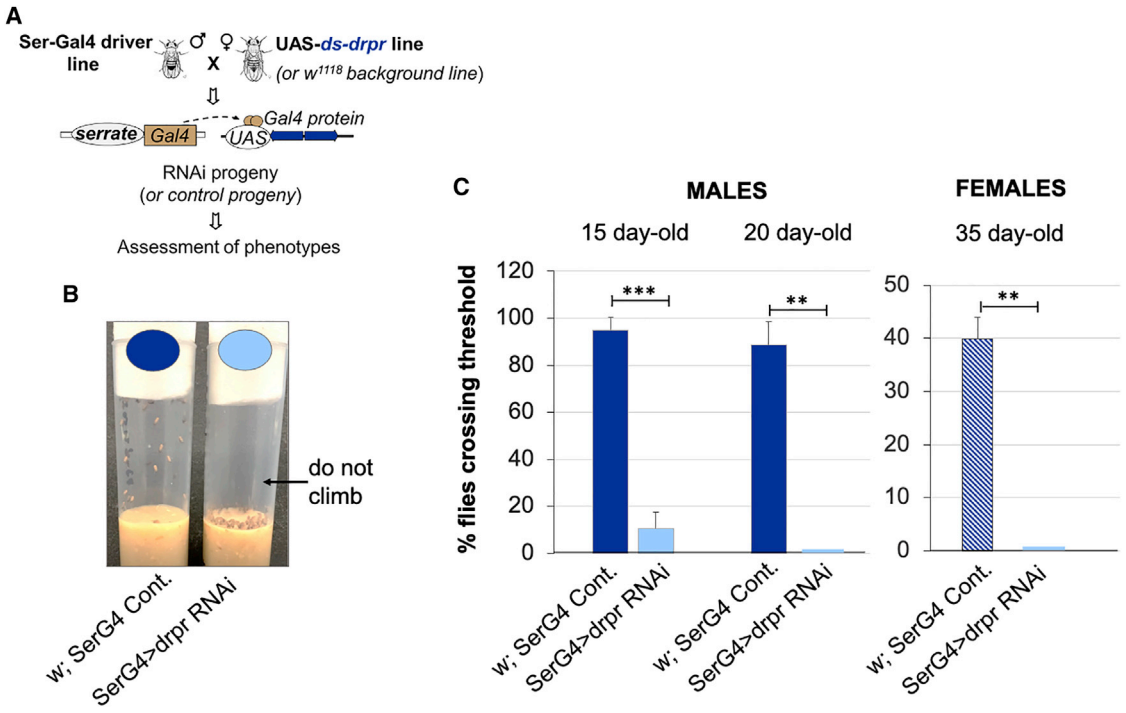

Figure 7. Adult *Drosophila* that downregulate *drpr/Megf10* in *serrate* (*Ser*)-positive cells display a marked defect in locomotor activity
(A) Schematic representation of the genetic crosses that were established to generate progeny expressing a *drpr* RNAi construct in the imaginal disc-associated serrate-positive cells (abbreviated genotype *SerG4 > drpr RNAi*). Corresponding control progeny were generated in parallel crosses (abbreviated genotype w^{1118}*; SerG4*). After emerging, adult RNAi and control flies were collected, sexed, aged, and functionally characterized.
(B) Negative geotaxis assay. The flies were prompted by tapping both vials simultaneously once on a flat surface and the climbing ability of the flies was video recorded. Representative still photographs are shown, and the full video is available as Video S1. Most control flies reached the top in less than 10 s, while *SerG4 > drpr RNAi* flies were unable to climb.
(C) Negative geotaxis assay quantification. *SerG4 > drpr* flies and w^{1118}*; SerG4* control flies were assessed for their ability to cross a 5 cm threshold line in 5 s. The assay was performed in triplicate/biological sample (n = 2–4 replicates of 10 to 15 flies each per genotype per sex). Values in the graph show mean ± SEM. Statistical significance, RNAi flies versus control flies via Student's t test, two-sample unequal variable: $^{**}p < 0.01$; $^{***}p < 0.001$.

muscular dystrophies (GEO: GSE109178; Duchenne muscular dystrophy [DMD], Becker muscular dystrophy [BMD], LGMD R2 dysferlin-related, LGMD R9 *FKRP*-related)[54] show upregulation of *PAX7* mRNA levels. Correspondingly, immunostaining for PAX7 and MYF5 in muscle biopsies from individuals with DMD revealed a higher number of satellite cells than in control biopsies, even at advanced stages of the disease.[55]

Our myoblast data indicate that several Notch pathway components that are known to interact with Jagged2 are significantly downregulated. Among these, Delta-like 1 and Jagged1 are particularly intriguing because the encoding human orthologous genes are also linked to Mendelian diseases, albeit with phenotypes that are strikingly different from *JAG2*-related muscular dystrophy. In golden retrievers with muscular dystrophy, higher levels of Jagged1 expression have been shown to ameliorate the phenotype,[56] suggesting that modulation of various Notch pathway components could have therapeutic potential for muscular dystrophy.

A mouse model of Jagged2 deficiency would help study these issues further. However, *Jag2* knockout mice experience early lethality due to cleft palate, limiting the utility of this mouse line for studies of skeletal muscle disease.[57] A $Jag2^{flox}$ allele has been generated to circumvent this obstacle.[58] Crossing $Jag2^{flox}$ mice with mice expressing the Cre recombinase under the control of a skeletal muscle-specific promoter could help to gain further insight in the role of *Jag2* in skeletal muscle in mice.

The *Drosophila* ortholog of mammalian *Jagged2* is *Serrate* (*Ser, CG6127*). Previous work in flies established that Serrate is expressed in the epidermal tissue of the wing imaginal disc and modulates Notch activity in the immediately adjacent adult muscle progenitors (AMPs) that form the disc myogenic layer. Serrate is required in *trans* to activate Notch signaling-dependent division/proliferation of the AMP lineage, from ten cells to about 2,500.[59] Expression of a *Ser*-RNAi construct targeted to muscle cells (i.e., *in cis* to Notch), however, does not affect myogenesis in flies.[60] Future studies of transgenic flies representing the pathogenic missense variants would help further elucidate the role of Serrate in muscle development and repair. In earlier studies, we and others have shown that another protein that interacts with the Notch pathway, mammalian Megf10/

Drosophila Drpr, plays an important role in muscle development.[61,62] Megf10/Drpr, like Jagged2/Ser, is a transmembrane protein that is associated with an inherited muscle disease.[19]

The current studies show that downregulation of Drpr in the discrete subset of Ser-positive wing disc cells leads to markedly diminished motor activity in adult flies. This observation suggests that although the two proteins may be co-expressed, Ser cannot compensate for the loss of Drpr. It is known that Ser-positive cells in the wing disc provide a critical and transient signaling niche to Notch, and that Ser expression fades when the AMPs initiate asymmetric division, prior to differentiation. The effects of Ser overexpression at different stages of myogenesis in *Drosophila* might provide additional insight on the role of this protein, as was shown for Drpr.[63] A marked increase in Jagged2 levels was seen after treating Megf10-deficient myoblasts with a candidate small molecule therapeutic,[62] bolstering our findings in participant muscle tissue and myoblasts.

The form of muscular dystrophy described here is associated with bi-allelic pathogenic variants in *JAG2* that are highly conserved across species and that predict protein loss of function on the basis of correlations with prior structural work for the encoded protein Jagged2. A spectrum of disease severity is associated with specific genotypes. There are intriguing clinical and biological features suggesting that *JAG2*-related muscular dystrophy shares a common Notch pathway-related disease mechanism with at least two other inherited muscle diseases, LGMD R21 *POGLUT1*-related and EMARDD. Future studies focusing on potential impacts of pathogenic variants in these genes on satellite cell function as well as potential interactions among their protein products promise to yield important knowledge with regard to muscle disease mechanisms and potential therapeutic targets.

Data and code availability

The transcriptome (RNA-seq) raw datasets are included as Tables S5 and S6 accompanying this article.

Supplemental information

Supplemental information can be found online at https://doi.org/10.1016/j.ajhg.2021.03.020.

Declaration of interests

The authors declare no competing interests.

Received: November 30, 2020
Accepted: March 26, 2021
Published: April 15, 2021; corrected online: April 28, 2021

Web resources

CADD, https://cadd.gs.washington.edu/snv
Clustal Omega, https://www.ebi.ac.uk/Tools/msa/clustalo/
gnomAD, https://gnomad.broadinstitute.org/
GTEx, https://gtexportal.org/home/
Illustrator for Biological sequences, http://ibs.biocuckoo.org/
Matchmaker Exchange, https://www.matchmakerexchange.org/
OMIM, https://omim.org/
UniProt, https://www.uniprot.org/
PyMol, https://pymol.org/2/
Vienna *Drosophila* Resource Center (VDRC), http://stockcenter.vdrc.at/

References

1. Straub, V., Murphy, A., Udd, B.; and LGMD workshop study group (2018). 229th ENMC international workshop: Limb girdle muscular dystrophies - Nomenclature and reformed classification Naarden, the Netherlands, 17-19 March 2017. Neuromuscul. Disord. *28*, 702–710.
2. Kang, P.B., Morrison, L., Iannaccone, S.T., Graham, R.J., Bönnemann, C.G., Rutkowski, A., Hornyak, J., Wang, C.H., North, K., Oskoui, M., et al. (2015). Evidence-based guideline summary: evaluation, diagnosis, and management of congenital muscular dystrophy: Report of the Guideline Development Subcommittee of the American Academy of Neurology and the Practice Issues Review Panel of the American Association of Neuromuscular & Electrodiagnostic Medicine. Neurology *84*, 1369–1378.
3. Nallamilli, B.R.R., Chakravorty, S., Kesari, A., Tanner, A., Ankala, A., Schneider, T., da Silva, C., Beadling, R., Alexander, J.J., Askree, S.H., et al. (2018). Genetic landscape and novel disease mechanisms from a large LGMD cohort of 4656 patients. Ann. Clin. Transl. Neurol. *5*, 1574–1587.
4. Reddy, H.M., Cho, K.-A., Lek, M., Estrella, E., Valkanas, E., Jones, M.D., Mitsuhashi, S., Darras, B.T., Amato, A.A., Lidov, H.G., et al. (2017). The sensitivity of exome sequencing in identifying pathogenic mutations for LGMD in the United States. J. Hum. Genet. *62*, 243–252.
5. Töpf, A., Johnson, K., Bates, A., Phillips, L., Chao, K.R., England, E.M., Laricchia, K.M., Mullen, T., Valkanas, E., Xu, L., et al. (2020). Sequential targeted exome sequencing of 1001 patients affected by unexplained limb-girdle weakness. Genet. Med. *22*, 1478–1488.
6. Mašek, J., and Andersson, E.R. (2017). The developmental biology of genetic Notch disorders. Development *144*, 1743–1763.
7. Mourikis, P., and Tajbakhsh, S. (2014). Distinct contextual roles for Notch signalling in skeletal muscle stem cells. BMC Dev. Biol. *14*, 2.
8. Suckling, R.J., Korona, B., Whiteman, P., Chillakuri, C., Holt, L., Handford, P.A., and Lea, S.M. (2017). Structural and functional dissection of the interplay between lipid and Notch binding by human Notch ligands. EMBO J. *36*, 2204–2215.
9. Guruharsha, K.G., Kankel, M.W., and Artavanis-Tsakonas, S. (2012). The Notch signalling system: recent insights into the complexity of a conserved pathway. Nat. Rev. Genet. *13*, 654–666.
10. Li, L., Krantz, I.D., Deng, Y., Genin, A., Banta, A.B., Collins, C.C., Qi, M., Trask, B.J., Kuo, W.L., Cochran, J., et al. (1997).

Alagille syndrome is caused by mutations in human Jagged1, which encodes a ligand for Notch1. Nat. Genet. *16*, 243–251.
11. Bauer, R.C., Laney, A.O., Smith, R., Gerfen, J., Morrissette, J.J.D., Woyciechowski, S., Garbarini, J., Loomes, K.M., Krantz, I.D., Urban, Z., et al. (2010). Jagged1 (JAG1) mutations in patients with tetralogy of Fallot or pulmonic stenosis. Hum. Mutat. *31*, 594–601.
12. Le Caignec, C., Lefevre, M., Schott, J.J., Chaventre, A., Gayet, M., Calais, C., and Moisan, J.P. (2002). Familial deafness, congenital heart defects, and posterior embryotoxon caused by cysteine substitution in the first epidermal-growth-factor-like domain of jagged 1. Am. J. Hum. Genet. *71*, 180–186.
13. Sullivan, J.M., Motley, W.W., Johnson, J.O., Aisenberg, W.H., Marshall, K.L., Barwick, K.E.S., Kong, L., Huh, J.S., Saavedra-Rivera, P.C., McEntagart, M.M., et al. (2020). Dominant mutations of the Notch ligand Jagged1 cause peripheral neuropathy. J. Clin. Invest. *130*, 1506–1512.
14. Fischer-Zirnsak, B., Segebrecht, L., Schubach, M., Charles, P., Alderman, E., Brown, K., Cadieux-Dion, M., Cartwright, T., Chen, Y., Costin, C., et al. (2019). Haploinsufficiency of the Notch Ligand DLL1 Causes Variable Neurodevelopmental Disorders. Am. J. Hum. Genet. *105*, 631–639.
15. Meester, J.A.N., Southgate, L., Stittrich, A.-B., Venselaar, H., Beekmans, S.J.A., den Hollander, N., Bijlsma, E.K., Helderman-van den Enden, A., Verheij, J.B., Glusman, G., et al. (2015). Heterozygous Loss-of-Function Mutations in DLL4 Cause Adams-Oliver Syndrome. Am. J. Hum. Genet. *97*, 475–482.
16. Bulman, M.P., Kusumi, K., Frayling, T.M., McKeown, C., Garrett, C., Lander, E.S., Krumlauf, R., Hattersley, A.T., Ellard, S., and Turnpenny, P.D. (2000). Mutations in the human delta homologue, DLL3, cause axial skeletal defects in spondylocostal dysostosis. Nat. Genet. *24*, 438–441.
17. Karczewski, K.J., Francioli, L.C., Tiao, G., Cummings, B.B., Alföldi, J., Wang, Q., Collins, R.L., Laricchia, K.M., Ganna, A., Birnbaum, D.P., et al. (2020). The mutational constraint spectrum quantified from variation in 141,456 humans. Nature *581*, 434–443.
18. Deng, Y., Madan, A., Banta, A.B., Friedman, C., Trask, B.J., Hood, L., and Li, L. (2000). Characterization, chromosomal localization, and the complete 30-kb DNA sequence of the human Jagged2 (JAG2) gene. Genomics *63*, 133–138.
19. Logan, C.V., Lucke, B., Pottinger, C., Abdelhamed, Z.A., Parry, D.A., Szymanska, K., Diggle, C.P., van Riesen, A., Morgan, J.E., Markham, G., et al. (2011). Mutations in MEGF10, a regulator of satellite cell myogenesis, cause early onset myopathy, areflexia, respiratory distress and dysphagia (EMARDD). Nat. Genet. *43*, 1189–1192.
20. Servián-Morilla, E., Takeuchi, H., Lee, T.V., Clarimon, J., Mavillard, F., Area-Gómez, E., Rivas, E., Nieto-González, J.L., Rivero, M.C., Cabrera-Serrano, M., et al. (2016). A POGLUT1 mutation causes a muscular dystrophy with reduced Notch signaling and satellite cell loss. EMBO Mol. Med. *8*, 1289–1309.
21. Philippakis, A.A., Azzariti, D.R., Beltran, S., Brookes, A.J., Brownstein, C.A., Brudno, M., Brunner, H.G., Buske, O.J., Carey, K., Doll, C., et al. (2015). The Matchmaker Exchange: a platform for rare disease gene discovery. Hum. Mutat. *36*, 915–921.
22. Dobin, A., Davis, C.A., Schlesinger, F., Drenkow, J., Zaleski, C., Jha, S., Batut, P., Chaisson, M., and Gingeras, T.R. (2013). STAR: ultrafast universal RNA-seq aligner. Bioinformatics *29*, 15–21.
23. Frankish, A., Diekhans, M., Ferreira, A.-M., Johnson, R., Jungreis, I., Loveland, J., Mudge, J.M., Sisu, C., Wright, J., Armstrong, J., et al. (2019). GENCODE reference annotation for the human and mouse genomes. Nucleic Acids Res. *47* (D1), D766–D773.
24. Brechtmann, F., Mertes, C., Matusevičiūtė, A., Yépez, V.A., Avsec, Ž., Herzog, M., Bader, D.M., Prokisch, H., and Gagneur, J. (2018). OUTRIDER: A Statistical Method for Detecting Aberrantly Expressed Genes in RNA Sequencing Data. Am. J. Hum. Genet. *103*, 907–917.
25. Szklarczyk, D., Gable, A.L., Lyon, D., Junge, A., Wyder, S., Huerta-Cepas, J., Simonovic, M., Doncheva, N.T., Morris, J.H., Bork, P., et al. (2019). STRING v11: protein-protein association networks with increased coverage, supporting functional discovery in genome-wide experimental datasets. Nucleic Acids Res. *47* (D1), D607–D613.
26. Draper, I., Mahoney, L.J., Mitsuhashi, S., Pacak, C.A., Salomon, R.N., and Kang, P.B. (2014). Silencing of drpr leads to muscle and brain degeneration in adult Drosophila. Am. J. Pathol. *184*, 2653–2661.
27. Chillakuri, C.R., Sheppard, D., Lea, S.M., and Handford, P.A. (2012). Notch receptor-ligand binding and activation: insights from molecular studies. Semin. Cell Dev. Biol. *23*, 421–428.
28. Gilbert, M.A., Bauer, R.C., Rajagopalan, R., Grochowski, C.M., Chao, G., McEldrew, D., Nassur, J.A., Rand, E.B., Krock, B.L., Kamath, B.M., et al. (2019). Alagille syndrome mutation update: Comprehensive overview of JAG1 and NOTCH2 mutation frequencies and insight into missense variant classification. Hum. Mutat. *40*, 2197–2220.
29. Kohsaka, T., Yuan, Z.-R., Guo, S.-X., Tagawa, M., Nakamura, A., Nakano, M., Kawasasaki, H., Inomata, Y., Tanaka, K., and Miyauchi, J. (2002). The significance of human jagged 1 mutations detected in severe cases of extrahepatic biliary atresia. Hepatology *36*, 904–912.
30. Hayward, C., and Brock, D.J. (1997). Fibrillin-1 mutations in Marfan syndrome and other type-1 fibrillinopathies. Hum. Mutat. *10*, 415–423.
31. Downing, A.K., Knott, V., Werner, J.M., Cardy, C.M., Campbell, I.D., and Handford, P.A. (1996). Solution structure of a pair of calcium-binding epidermal growth factor-like domains: implications for the Marfan syndrome and other genetic disorders. Cell *85*, 597–605.
32. Appella, E., Weber, I.T., and Blasi, F. (1988). Structure and function of epidermal growth factor-like regions in proteins. FEBS Lett. *231*, 1–4.
33. Mercuri, E., Lampe, A., Allsop, J., Knight, R., Pane, M., Kinali, M., Bönnemann, C., Flanigan, K., Lapini, I., Bushby, K., et al. (2005). Muscle MRI in Ullrich congenital muscular dystrophy and Bethlem myopathy. Neuromuscul. Disord. *15*, 303–310.
34. Barp, A., Laforet, P., Bello, L., Tasca, G., Vissing, J., Monforte, M., Ricci, E., Choumert, A., Stojkovic, T., Malfatti, E., et al. (2020). European muscle MRI study in limb girdle muscular dystrophy type R1/2A (LGMDR1/LGMD2A). J. Neurol. *267*, 45–56.
35. Fu, J., Zheng, Y.-M., Jin, S.-Q., Yi, J.-F., Liu, X.-J., Lyn, H., Wang, Z.-X., Zhang, W., Xiao, J.-X., and Yuan, Y. (2016). "Target" and "Sandwich" Signs in Thigh Muscles have High Diagnostic Values for Collagen VI-related Myopathies. Chin. Med. J. (Engl.) *129*, 1811–1816.
36. Ellgaard, L., and Helenius, A. (2003). Quality control in the endoplasmic reticulum. Nat. Rev. Mol. Cell Biol. *4*, 181–191.

37. Ladi, E., Nichols, J.T., Ge, W., Miyamoto, A., Yao, C., Yang, L.-T., Boulter, J., Sun, Y.E., Kintner, C., and Weinmaster, G. (2005). The divergent DSL ligand Dll3 does not activate Notch signaling but cell autonomously attenuates signaling induced by other DSL ligands. J. Cell Biol. *170*, 983–992.
38. Chapman, G., Sparrow, D.B., Kremmer, E., and Dunwoodie, S.L. (2011). Notch inhibition by the ligand DELTA-LIKE 3 defines the mechanism of abnormal vertebral segmentation in spondylocostal dysostosis. Hum. Mol. Genet. *20*, 905–916.
39. Servián-Morilla, E., Cabrera-Serrano, M., Johnson, K., Pandey, A., Ito, A., Rivas, E., Chamova, T., Muelas, N., Mongini, T., Nafissi, S., et al. (2020). POGLUT1 biallelic mutations cause myopathy with reduced satellite cells, α-dystroglycan hypoglycosylation and a distinctive radiological pattern. Acta Neuropathol. *139*, 565–582.
40. Boyden, S.E., Mahoney, L.J., Kawahara, G., Myers, J.A., Mitsuhashi, S., Estrella, E.A., Duncan, A.R., Dey, F., DeChene, E.T., Blasko-Goehringer, J.M., et al. (2012). Mutations in the satellite cell gene MEGF10 cause a recessive congenital myopathy with minicores. Neurogenetics *13*, 115–124.
41. Pierson, T.M., Markello, T., Accardi, J., Wolfe, L., Adams, D., Sincan, M., Tarazi, N.M., Fajardo, K.F., Cherukuri, P.F., Bajraktari, I., et al. (2013). Novel SNP array analysis and exome sequencing detect a homozygous exon 7 deletion of MEGF10 causing early onset myopathy, areflexia, respiratory distress and dysphagia (EMARDD). Neuromuscul. Disord. *23*, 483–488.
42. Harris, E., Marini-Bettolo, C., Töpf, A., Barresi, R., Polvikovski, T., Bailey, G., Charlton, R., Tellez, J., MacArthur, D., Guglieri, M., et al. (2018). MEGF10 related myopathies: a new case with adult onset disease with prominent respiratory failure and review of reported phenotypes. Neuromuscul. Disord. *28*, 48–53.
43. Mauro, A. (1961). Satellite cell of skeletal muscle fibers. J. Biophys. Biochem. Cytol. *9*, 493–495.
44. Sambasivan, R., Yao, R., Kissenpfennig, A., Van Wittenberghe, L., Paldi, A., Gayraud-Morel, B., Guenou, H., Malissen, B., Tajbakhsh, S., and Galy, A. (2011). Pax7-expressing satellite cells are indispensable for adult skeletal muscle regeneration. Development *138*, 3647–3656.
45. Bjornson, C.R.R., Cheung, T.H., Liu, L., Tripathi, P.V., Steeper, K.M., and Rando, T.A. (2012). Notch signaling is necessary to maintain quiescence in adult muscle stem cells. Stem Cells *30*, 232–242.
46. Mourikis, P., Sambasivan, R., Castel, D., Rocheteau, P., Bizzarro, V., and Tajbakhsh, S. (2012). A critical requirement for notch signaling in maintenance of the quiescent skeletal muscle stem cell state. Stem Cells *30*, 243–252.
47. Fujimaki, S., Seko, D., Kitajima, Y., Yoshioka, K., Tsuchiya, Y., Masuda, S., and Ono, Y. (2018). Notch1 and Notch2 Coordinately Regulate Stem Cell Function in the Quiescent and Activated States of Muscle Satellite Cells. Stem Cells *36*, 278–285.
48. De Micheli, A.J., Spector, J.A., Elemento, O., and Cosgrove, B.D. (2020). A reference single-cell transcriptomic atlas of human skeletal muscle tissue reveals bifurcated muscle stem cell populations. Skelet. Muscle *10*, 19.
49. Verma, M., Asakura, Y., Murakonda, B.S.R., Pengo, T., Latroche, C., Chazaud, B., McLoon, L.K., and Asakura, A. (2018). Muscle Satellite Cell Cross-Talk with a Vascular Niche Maintains Quiescence via VEGF and Notch Signaling. Cell Stem Cell *23*, 530–543.e9.
50. Gayraud-Morel, B., Chrétien, F., Jory, A., Sambasivan, R., Negroni, E., Flamant, P., Soubigou, G., Coppée, J.-Y., Di Santo, J., Cumano, A., et al. (2012). Myf5 haploinsufficiency reveals distinct cell fate potentials for adult skeletal muscle stem cells. J. Cell Sci. *125*, 1738–1749.
51. Feichtinger, R.G., Mucha, B.E., Hengel, H., Orfi, Z., Makowski, C., Dort, J., D'Anjou, G., Nguyen, T.T.M., Buchert, R., Juenger, H., et al. (2019). Biallelic variants in the transcription factor PAX7 are a new genetic cause of myopathy. Genet. Med. *21*, 2521–2531.
52. Castets, P., Bertrand, A.T., Beuvin, M., Ferry, A., Le Grand, F., Castets, M., Chazot, G., Rederstorff, M., Krol, A., Lescure, A., et al. (2011). Satellite cell loss and impaired muscle regeneration in selenoprotein N deficiency. Hum. Mol. Genet. *20*, 694–704.
53. Servián-Morilla, E., Cabrera-Serrano, M., Rivas-Infante, E., Carvajal, A., Lamont, P.J., Pelayo-Negro, A.L., Ravenscroft, G., Junckerstorff, R., Dyke, J.M., Fletcher, S., et al. (2019). Altered myogenesis and premature senescence underlie human TRIM32-related myopathy. Acta. Neuropathol. Commun. *7*, 30.
54. Dadgar, S., Wang, Z., Johnston, H., Kesari, A., Nagaraju, K., Chen, Y.-W., Hill, D.A., Partridge, T.A., Giri, M., Freishtat, R.J., et al. (2014). Asynchronous remodeling is a driver of failed regeneration in Duchenne muscular dystrophy. J. Cell Biol. *207*, 139–158.
55. Kottlors, M., and Kirschner, J. (2010). Elevated satellite cell number in Duchenne muscular dystrophy. Cell Tissue Res. *340*, 541–548.
56. Vieira, N.M., Elvers, I., Alexander, M.S., Moreira, Y.B., Eran, A., Gomes, J.P., Marshall, J.L., Karlsson, E.K., Verjovski-Almeida, S., Lindblad-Toh, K., et al. (2015). Jagged 1 Rescues the Duchenne Muscular Dystrophy Phenotype. Cell *163*, 1204–1213.
57. Jiang, R., Lan, Y., Chapman, H.D., Shawber, C., Norton, C.R., Serreze, D.V., Weinmaster, G., and Gridley, T. (1998). Defects in limb, craniofacial, and thymic development in Jagged2 mutant mice. Genes Dev. *12*, 1046–1057.
58. Xu, J., Krebs, L.T., and Gridley, T. (2010). Generation of mice with a conditional null allele of the Jagged2 gene. Genesis *48*, 390–393.
59. Gunage, R.D., Reichert, H., and VijayRaghavan, K. (2014). Identification of a new stem cell population that generates Drosophila flight muscles. eLife *3*, e03126.
60. Schnorrer, F., Schönbauer, C., Langer, C.C.H., Dietzl, G., Novatchkova, M., Schernhuber, K., Fellner, M., Azaryan, A., Radolf, M., Stark, A., et al. (2010). Systematic genetic analysis of muscle morphogenesis and function in Drosophila. Nature *464*, 287–291.
61. Holterman, C.E., Le Grand, F., Kuang, S., Seale, P., and Rudnicki, M.A. (2007). Megf10 regulates the progression of the satellite cell myogenic program. J. Cell Biol. *179*, 911–922.
62. Saha, M., Mitsuhashi, S., Jones, M.D., Manko, K., Reddy, H.M., Bruels, C.C., Cho, K.-A., Pacak, C.A., Draper, I., and Kang, P.B. (2017). Consequences of MEGF10 deficiency on myoblast function and Notch1 interactions. Hum. Mol. Genet. *26*, 2984–3000.
63. Draper, I., Saha, M., Stonebreaker, H., Salomon, R.N., Matin, B., and Kang, P.B. (2019). The impact of Megf10/Drpr gain-of-function on muscle development in Drosophila. FEBS Lett. *593*, 680–696.